International Geology Review, Vol. 48, 2006, p. 223–240.

Granitic Magmatism in the North Qaidam Early Paleozoic Ultrahigh-Pressure Metamorphic Belt, Northwest China

WU CAILAI,[1]

Continental Dynamics Laboratory, Institute of Geology, Chinese Academy of Geological Sciences, Beijing, 100037 China

JOSEPH L. WOODEN,

Department of Earth and Environmental Sciences, Stanford University, Stanford, California 94305

YANG JINGSUI,

Continental Dynamics Laboratory, Institute of Geology, Chinese Academy of Geological Sciences, Beijing, 100037 China

PAUL T. ROBINSON,

Department of Earth Sciences, Dalhousie University, Halifax, Nova Scotia, Canada B3H 3J5

ZHENG LINGSEN, SHI RENDENG, AND CHEN SONGYONG

Continental Dynamics Laboratory, Institute of Geology, Chinese Academy of Geological Sciences, Beijing, 100037 China

Abstract

Three suites of granitic rocks are present in the early Paleozoic North Qaidam ultrahigh-pressure (UHP) metamorphic belt, which has eclogite ages of 466–495 Ma. The first suite consists of quartz monzodiorite + granodiorite + monzogranite, the second of monzogranite + two-mica granite + muscovite granite + syenogranite, and the third of granodiorite + monzogranite + biotite granite. The country rocks into which these bodies were intruded consist chiefly of medium- and high-grade Proterozoic gneisses and schists and Paleozoic sedimentary and volcanic rocks. Monzogranite of the first suite has a zircon SHRIMP age of 473 Ma, whereas syenogranite in the second suite has an age of 446 Ma, and granodiorite in the third suite has an age of 397 Ma. Rocks of the first and third suites have similar mineralogies consisting of plagioclase, hornblende, quartz, alkali feldspar, and biotite, whereas those of the second suite consist of potassium feldspar, quartz, muscovite, biotite, and plagioclase. Rocks of the first and third suites have I-type compositions with SiO2 = 61–69 wt%, Na_2O/K_2O >1, ANK <1, and Eu/Eu* = 0.7–1.0, whereas the second suite consists of S-type granites, with SiO_2 = 70–76 wt%, Na_2O/K_2O <1, ANK >1, and Eu/Eu* = 0.1–0.3. The first suite is interpreted as island arc or active continental margin magmatism, the second as igneous activity related to collision between the Qaidam and Qilian blocks, and the third as post-collisional plutonic activity.

Introduction

THE NORTH QAIDAM terrane of northwest China is a long, narrow mountain range extending southeastward from Altyn to Aloitoshan, a distance of about 800 km (Fig. 1). It is a fold belt composed mainly of Proterozoic and Paleozoic rocks. The Proterozoic basement consists of intermediate- and high-grade gneisses and schists with ages of 1463–1617 Ma, ultrabasic rocks and newly discovered diamond- and coesite-bearing eclogites (BGMRQH, 1991; Yang et al., 1998). The Lower Paleozoic sequences consist mainly of strongly deformed Ordovician deep marine sedimentary and volcanic rocks, overlain by Upper Devonian continental clastic and volcanic rocks and Carboniferous shallow-marine sedimentary rocks. Early Paleozoic to Mesozoic granitoids are widespread in the region (BGMRQH, 1991).

The North Qaidam is considered to be a suture zone that separates the Qilian terrane from the Qaidam massif, and thus holds crucial information on the tectonics of northwest China. Unfortunately, little is known about the geological, petrological, and geochemical character of this belt, particularly the widespread granitoids. In this study, we investigated North Qaidam granitoids in order to under-

[1]Corresponding author; email:wucalai@hotmail.com

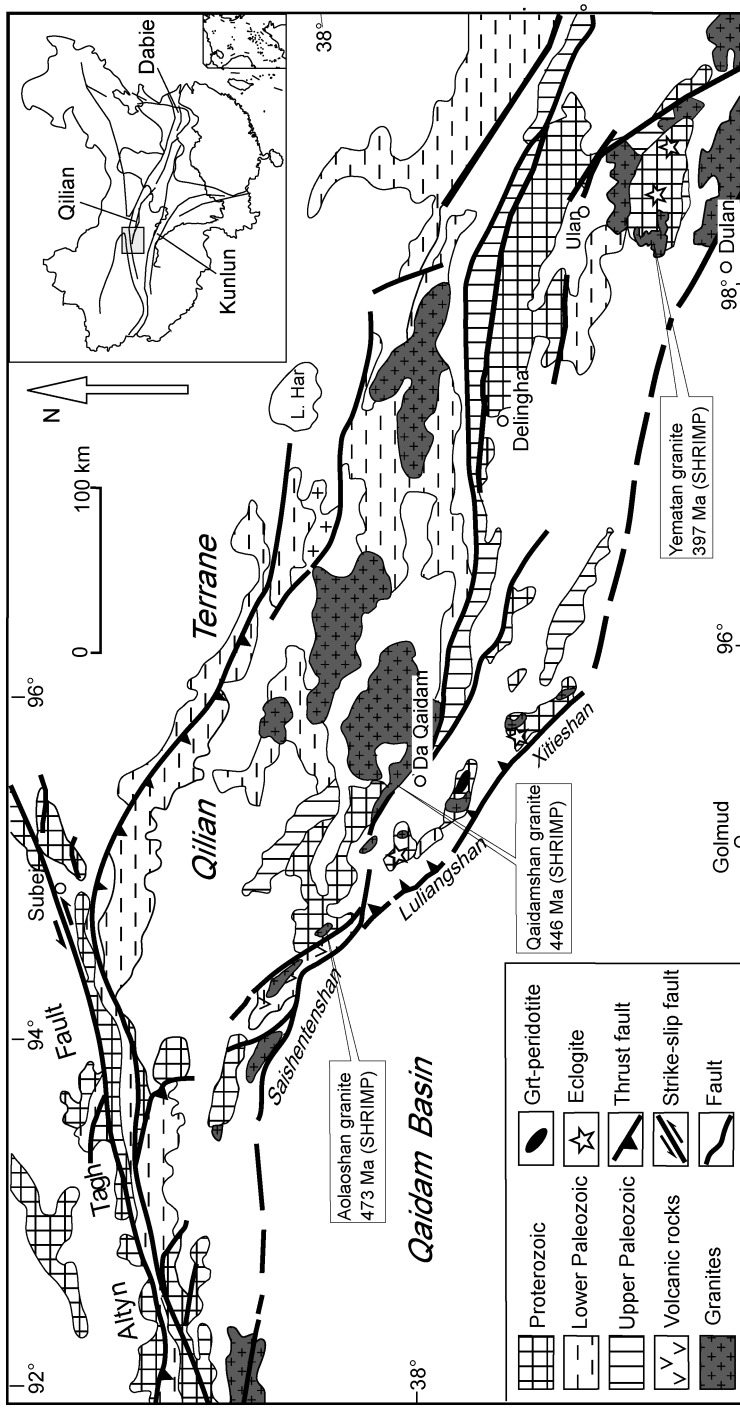

FIG. 1. Geological sketch map of North Qaidam.

stand better the nature of the plutonism and how it relates to the tectonic evolution of the suture zone.

A number of granitoids with ages ranging from early Paleozoic to Mesozoic (BGMRQH, 1991) intrude the metasedimentary and metavolcanic rocks of North Qaidam, but few of them have been dated precisely. In 1998, eclogites were discovered in the Proterozoic gneisses of the Dakendaban group in Da Qaidan, and similar rocks have now been found at Luliangshan, Xitieshan, Dulan, and western Altun. These discoveries demonstrate that North Qaidam is part of a Paleozoic UHP metamorphic belt that stretches nearly 4000 km across northern China (Yang et al., 2000, 2001, 2002; Song et al., 2003a, 2003b). Eclogites from the region formed at peak pressures of more than 28 kbar, and have U/Pb zircon ages ranging from 445 to 500 Ma (Yang et al., 1998; Zhang et al., 1999). Coesite occurs as inclusions in zircons from the gneisses hosting the eclogites in Dulan (Yang et al., 2001, Song et al., 2003b). However, the relationship between the granites and the ultrahigh-pressure metamorphic rocks, and the tectonics of the UHP belt are still unclear. In this study, we carried out detailed geochemical studies and zircon SHRIMP dating of the granitoids of North Qaidam to: (1) characterize the geochemical nature of the granitoids; (2) tightly constrain their ages; and (3) investigate the relationship between the granitoids and the nearby UHP metamorphic rocks.

Lithology

Granitoid intrusives such as Saishentenshan, Aolaoshan, Yukahe, Luliangshan, Da Qaidam, Qaidamshan, Xitieshan, and Dulan Yematan occur widely in the North Qaidam belt. These bodies intrude intermediate- and high-grade metamorphic gneisses of Proterozoic age. Most of these granitoids, including Saishentenshan, Aolaoshan, and Xitieshan, form small dikes and apophyses, but a few, such as Qaidamshan and Dulan Yematan, are batholiths. The intrusions typically have sharp boundaries with the country rock, although some show evidence of interaction with the host material. In general, the intrusions lie along a northwest trend, and are aligned at a small angle to regional structures, indicating emplacement in a transpressional environment.

The granitic rocks from North Qaidam are chiefly syenogranite, monzogranite, and granodiorite, with minor quartz monzodiorite. Some of the rocks contain abundant biotite or muscovite. Based on their field occurrences and relationships, the granitoids fall into three series. The first, including the Aolaoshan and Luliangshan plutons, consists of quartz monzodiorite, granodiorite, and monzogranite, whereas the second series, represented by the Yuka and Qaidamshan intrusions, is composed of monzogranite, two-mica granite, muscovite granite, and orthogranite. The Saishentenshan, Xitieshan, and Dulan Yemata intrusives, composed of granodiorite, monzogranite, and biotite granite, represent the third series. Granitoids of the first and third series have similar mineral assemblages, consisting of plagioclase (40–60 modal%), quartz (5–20 modal%), hornblende (5–15 modal%), K-feldspar (3–10 modal%) and biotite (0–7 modal%). Rocks of the second series are more alkaline in composition and consist of K-feldspar (20–35 modal%), quartz (15–30 modal%), plagioclase (10–30 modal%), muscovite (0–8 modal%), biotite (0–7modal%), and sparse garnet (0–2 modal%). The first series is characterized by abundant plagioclase and hornblende, the second by alkaline feldspar and quartz with minor muscovite and garnet, and the third by a preponderance of biotite over hornblende.

Geochemistry

The chemical analyses were carried out at the National Geological Measurement Center, Chinese Academy of Geological Sciences, Beijing. Major oxides and some trace elements (Sr, Ba, Zn, Rb, Nb, Zr, and Ga) were determined by X-ray fluorescence spectrometry using the procedures outlined in GB/T14506-28-1993. Rare-earth elements (REE) and Y, Cu, Pb, Th, U, Hf, Ta, Sc, Cs, V, Co, and Ni were determined by plasma mass spectrometry (POEMS) and plasma ion spectrometry, following the procedures in GB/T0223-2001. Chemical compositions of the North Qaidam granitoids are listed in Table 1. These rocks have a wide range of composition with SiO_2 = 52.94–79.42 wt%, Na_2O+K_2O = 4.70–8.38 wt%, and Na_2O/K_2O = 1.07–3.70, with an average of 1.88. The granitoids of the first and third series are intermediate in composition, with SiO_2 ranging from 52.94 to 76.19 wt%, whereas those of the second series are much more silicic (SiO_2 = 73.05–79.42 wt%). All of the rocks belong to the subalkaline series as defined by Irvine (1971). Granitoids of the first and third series are calc-alkaline, whereas those of the second series are more potassic.

The total REE contents of the granitoids range from 61.9 to 258.6 ppm (Fig. 2). Rocks of the first

TABLE 1. Major and Trace Element Geochemistry of North Qaidam Granitoids

Locations:	Aolaoshan							Luliangshan	South Yukahe	West Da Qaidan		Qaidamshan
Samples:	k55-11	k55-15	k55-5	k55-6	k55-8	k55-13	k55-16	31-9	30-8	32-11	30-2a	32-43
SiO_2	52.94	55.57	68.50	71.34	71.86	70.68	71.90	73.36	73.05	74.11	76.06	74.51
TiO_2	1.07	0.87	0.47	0.24	0.21	0.29	0.23	0.14	0.22	0.11	0.20	0.26
Al_2O_3	17.77	16.33	15.11	15.05	14.66	14.63	14.36	14.37	14.08	14.16	14.24	12.34
Fe_2O_3	1.81	1.84	1.27	0.74	0.75	0.78	0.71	0.51	0.75	0.41	0.26	0.77
FeO	5.77	5.22	2.39	1.58	1.31	1.81	1.43	0.76	1.22	0.80	0.75	1.62
MnO	0.09	0.10	0.05	0.04	0.04	0.03	0.04	0.03	0.03	0.03	0.03	0.04
MgO	5.30	5.82	1.11	0.75	0.66	0.80	0.64	0.42	0.42	0.17	0.19	0.33
CaO	7.80	8.30	3.75	2.66	2.24	2.79	2.00	1.53	0.79	0.83	1.93	1.27
Na_2O	4.12	3.70	4.01	4.11	3.92	4.19	4.27	3.88	2.85	2.86	4.20	2.20
K_2O	1.41	1.00	2.33	2.73	3.67	2.86	3.36	2.84	5.11	5.52	2.09	5.82
P_2O_5	0.09	0.09	0.09	0.09	0.09	0.09	0.09	0.04	0.15	0.10	0.15	0.21
LOI	1.84	1.44	0.90	0.98	0.84	0.88	0.82	2.35	1.30	0.85	0.51	0.46
Total	100.01	100.28	99.98	100.31	100.25	99.83	99.85	100.23	99.97	99.95	100.61	99.83
Alk	5.53	4.70	6.34	6.84	7.59	7.05	7.63	6.72	7.96	8.38	6.29	8.02
Na/K	2.92	3.70	1.72	1.51	1.07	1.47	1.27	1.37	0.56	0.52	2.01	0.38
Rittimann	3.08	1.76	1.58	1.65	2.00	1.80	2.01	1.49	2.11	2.26	1.20	2.04
A/NKC	0.79	0.73	0.95	1.03	1.01	0.97	1.00	1.02	1.21	1.16	1.12	1.01
La	25.40	26.10	30.30	36.10	38.00	22.10	35.20	15.66	47.55	19.12	35.30	37.67
Ce	52.80	51.20	53.30	53.50	57.40	40.80	54.50	25.32	87.56	33.76	70.76	72.56
Pr	5.30	5.14	5.29	5.24	5.19	3.64	4.46	2.88	9.95	3.74	7.67	7.95
Nd	26.90	23.20	21.90	20.10	21.30	15.30	18.40	10.00	33.27	12.96	26.87	29.50
Sm	6.03	4.93	4.79	3.68	3.46	2.82	3.07	2.36	7.63	3.49	7.22	8.23
Eu	1.45	1.17	1.03	0.87	0.88	0.77	0.67	0.65	0.71	0.45	0.60	0.94
Gd	5.88	5.06	5.29	2.65	3.13	2.60	1.92	1.91	5.68	3.54	6.80	8.37
Tb	1.05	0.71	0.60	0.48	0.37	0.19	0.26	3.0	0.85	0.65	1.09	1.38
Dy	6.00	4.32	4.25	2.96	2.54	1.75	2.09	1.32	4.34	3.67	5.69	7.82
Ho	1.30	0.75	0.77	0.45	0.28	0.23	0.37	0.27	0.77	0.71	1.13	1.42
Er	3.44	2.48	2.75	1.84	1.62	1.24	1.40	0.72	2.15	2.05	2.87	3.11
Tm	0.42	0.23	0.36	0.21	0.19	0.12	0.18	0.11	0.30	0.32	0.38	0.34
Yb	2.71	1.70	2.29	1.29	0.97	0.71	0.90	0.67	1.91	2.09	2.04	1.84
Lu	0.33	0.26	0.32	0.27	0.07	0.10	0.13	0.09	0.28	0.32	0.36	0.36
REE	139.0	127.3	133.2	129.6	135.4	92.4	123.6	62.3	203.0	86.9	168.8	181.5
LRE/HRE	5.6	7.2	7.0	11.8	13.8	12.3	16.0	10.6	11.5	5.5	7.3	6.4
Eu/Eu*	0.7	0.7	0.6	0.8	0.8	0.9	0.8	0.9	0.3	0.4	0.3	0.3
Y	19.7	43.5	30.2	27.3	21.4	35.7	29.5	14.3	47.1	11.2	24.0	25.5
Rb	294	404	80	116	282	168	376	80.8	404	92.6	86.9	48.6
Sr	60	29	263	906	54	170	24.9	434	27.6	392	263	310
Ba	228	148	130	638	376	557	146	1254	124	1164	516	387
Nb	9.0	9.8	10.0	14.0	15.0	8.0	14.9	4.9	13.1	4.5	4.2	5.9
Ta	1.5	0.4	1.4	2.1	3.6	2.9	0.9	0.2	0.8	0.3	0.6	0.4
Zr	77.0	96.6	50.0	113.0	91.0	89.0	118.0	60.9	72.0	58.4	87.7	96.6
Hf	0.7	1.2	1.7	4.7	1.5	2.1	1.9	0.9	1.5	0.7	0.6	1.0
U	5.9	4.3	4.4	14.9	5.4	1.3	4.5	0.6	5.4	0.3	0.7	1.0
Th	16.7	50.7	25.8	54.9	27.4	22.0	47.0	4.5	39.0	4.0	9.7	8.8
V	1.8	13.0	13.4	198.0	18.5	10.2	12.7	21.6	11.8	19.9	42.6	69.5
Cr	1.7	21.6	3.3	60.6	9.2	22.0	25.6	40.7	22.9	31.9	28.5	77.3
Co	1.8	2.0	2.6	36.0	3.2	5.1	2.4	5.0	2.3	4.1	8.1	20.5
Ni	1.5	2.6	2.5	24.4	2.4	3.5	3.0	4.8	2.3	4.2	6.5	22.2

Table continues

TABLE 1. *Continued*

Location:	Qaidamshan				Saishentenshan				Xitieshan		Yematan	
Sample:	k55-1	k55-2	k55-3	k55-4	19-22	19-26	19-28	19-30	Z01-17-1	Z01-17-3	cl99-38	cl99-40
SiO_2	76.95	79.42	78.77	78.36	65.19	63.13	64.69	64.89	69.64	69.61	76.19	66.65
TiO_2	0.19	0.21	0.14	0.17	0.62	0.73	0.67	0.65	0.40	0.40	0.38	0.5
Al_2O_3	11.11	10.29	10.76	10.71	15.57	16.35	15.61	15.68	14.86	14.78	12.24	15.01
Fe_2O_3	0.58	0.46	0.46	0.59	1.43	1.48	1.81	2.17	0.65	0.41	0.35	0.71
FeO	1.11	1.42	1.11	1.10	2.40	2.78	2.14	2.01	1.89	1.99	0.7	3.47
MnO	0.02	0.03	0.02	0.02	0.08	0.07	0.07	0.06	0.06	0.05	0.15	2.11
MgO	0.24	0.26	0.15	0.20	2.39	2.89	2.50	2.62	1.08	0.98	0.02	0.12
CaO	0.65	0.67	0.53	0.63	4.37	4.72	4.38	4.67	2.51	2.62	0.78	3.94
Na_2O	2.30	2.26	2.64	2.51	4.27	4.42	4.24	4.59	3.57	3.69	2.62	3.86
K_2O	5.70	4.80	4.87	4.99	1.81	1.67	1.87	1.88	3.72	3.77	6.19	2.48
P_2O_5	0.09	0.09	0.09	0.09	0.14	0.17	0.15	0.15	0.10	0.11	0.07	0.09
LOI	0.56	0.60	0.54	0.52	1.19	1.53	1.41	0.78	0.94	0.74	0.16	0.94
Total	99.50	100.51	100.08	99.89	99.46	99.94	99.54	100.15	99.42	99.15	99.85	99.88
Alk	8.00	7.06	7.51	7.50	6.08	6.09	6.11	6.47	7.29	7.46	8.81	6.34
Na/K	0.40	0.47	0.54	0.50	2.36	2.65	2.27	2.44	0.96	0.98	0.42	1.56
Rittimann	1.89	1.37	1.58	1.59	1.67	1.84	1.72	1.91	1.99	2.09	2.34	1.70
A/NKC	1.00	1.01	1.02	1.00	0.92	0.92	0.92	0.87	1.03	0.99	0.98	0.93
La	59.20	61.00	47.90	59.00	16.43	15.34	16.51	15.11	38.01	40.73	11.1	20
Ce	112.00	113.00	89.80	108.00	32.37	34.61	33.85	30.48	72.38	74.46	31	45.3
Pr	10.50	10.40	8.53	10.00	3.82	3.44	3.68	3.56	6.92	7.03	3.02	5.45
Nd	39.60	40.00	34.90	40.10	14.77	15.33	15.45	13.59	23.90	24.67	9.54	20.7
Sm	8.39	7.78	8.16	9.00	3.83	3.84	3.84	3.28	3.68	3.37	1.82	5.15
Eu	0.35	0.35	0.38	0.45	0.82	1.03	0.99	0.82	0.83	0.83	0.54	1.1
Gd	7.60	7.12	8.71	9.73	2.74	2.51	2.89	2.59	3.05	3.09	1.6	3.44
Tb	1.47	1.12	1.88	1.47	0.50	0.44	0.50	0.43	0.44	0.41	0.21	0.59
Dy	8.45	6.33	11.10	9.02	2.63	2.69	2.69	2.37	2.04	1.85	1.12	3.72
Ho	1.71	1.13	2.44	1.86	0.60	0.55	0.54	0.50	0.34	0.34	0.27	0.93
Er	4.60	3.19	6.40	4.86	1.62	1.74	1.62	1.45	0.96	0.92	0.64	2.06
Tm	0.64	0.44	0.98	0.70	0.23	0.22	0.23	0.20	0.14	0.13	0.13	0.34
Yb	3.47	2.21	5.59	3.79	1.44	1.43	1.49	1.27	0.87	0.79	0.75	2.02
Lu	0.58	0.44	0.68	0.65	0.21	0.20	0.21	0.17	0.13	0.11	0.16	0.3
REE	258.6	254.5	227.4	258.6	82.0	83.4	84.5	75.8	153.7	158.7	61.9	111.1
LREE/HREE	8.1	10.6	5.0	7.1	7.2	7.5	7.3	7.4	18.3	19.8	11.7	7.3
Eu/Eu*	0.1	0.1	0.1	0.2	0.7	1.0	0.9	0.8	0.7	0.8	1.0	0.8
Y	31.0	7.4	20.3	9.3	15.3	15.4	15.6	14.0	5.0	27.5	8.5	13.7
Rb	43.8	68.1	34	63.8	50	47	54	58	186	124	161	130
Sr	393	342	291	324	322	363	337	339	171	289	366	509
Ba	387	757	367	1523	181	209	181	187	308	279	647	979
Nb	7.3	2.0	5.8	6.2	4.0	4.0	4.0	4.0	2.9	13.4	9.4	11.0
Ta	0.4	0.1	0.7	0.4	0.6	0.5	0.6	0.5	0.5	1.0	0.5	0.5
Zr	88.1	80.7	65.1	60.1	125	91	139	109	88.2	131	141	159
Hf	0.9	0.4	1.0	0.8	2.7	6.0	4.2	2.7	3.6	3.9	3.9	4.2
U	0.8	0.4	0.4	0.8	1.9	1.3	0.9	0.8	3.2	2.4	5.0	5.6
Th	3.3	6.4	1.5	7.0	7.0	5.0	6.7	6.0	34.0	17.0	22.0	21.0
V	101	25	97.4	4.96	81.2	67	57	65	4.7	71	31	53
Cr	53.2	28.5	242	0.82	50.4	57.8	53.8	75.7	6	27	17	18
Co	31.7	4.4	30.9	3.45	12.3	10	10	12	0.3	8.2	5.5	8.1
Ni	42.4	4.3	35.7	3.7	37.1	16.0	20.0	23.0	3.9	6.4	4.1	7.4

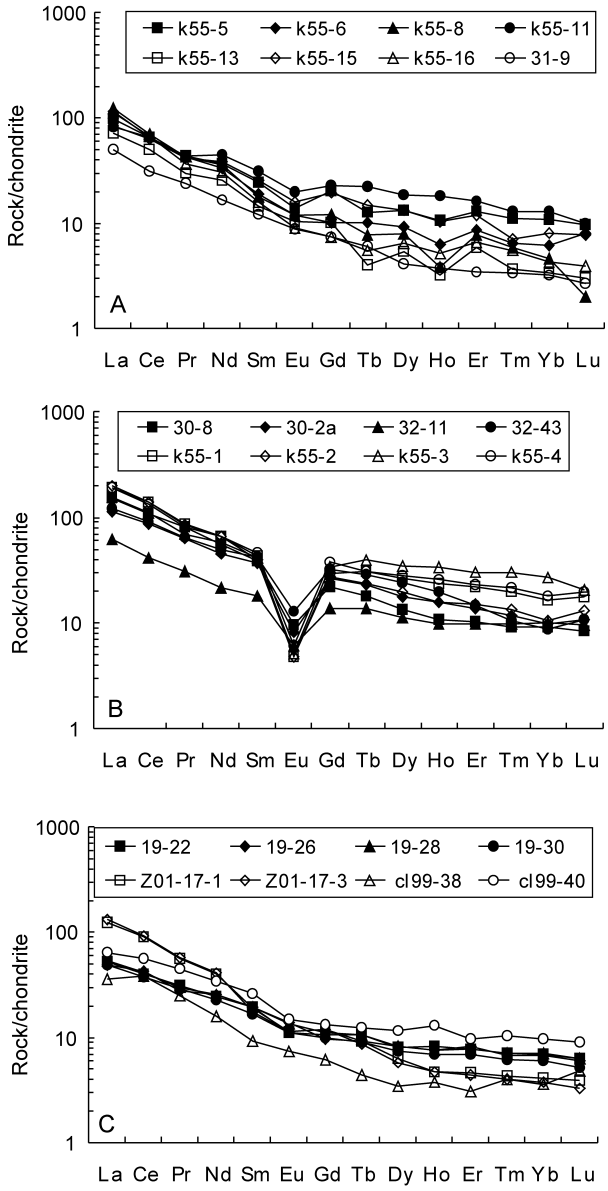

FIG. 2. Chondrite-normalized REE patterns of granitoids from North Qadaim. A, B, and C represent series 1, 2, and 3, respectively (chondrite values from Boynton, 1984).

and third series have total REE ranging from 61.9 to 158.7 ppm, LREE/HREE ratios ranging from 5.6 to 19.8, and Eu/Eu* ratios ranging from 0.6 to 1.0, whereas the rocks of the second series have total REE ranging from 86.9 to 258.6 ppm, LREE/HREE ratios of 5.0–11.5, and Eu/Eu* ratios from 0.1 to 0.4. In chondrite-normalized REE diagrams, the granitoids of the first and third series show LREE enrichment and have slightly negative Eu anomalies, whereas those of the second series have more distinct Eu anomalies.

Granitoids of the three different series show distinct trace element signatures (Fig. 3). In mantle-normalized trace element diagrams, rocks of

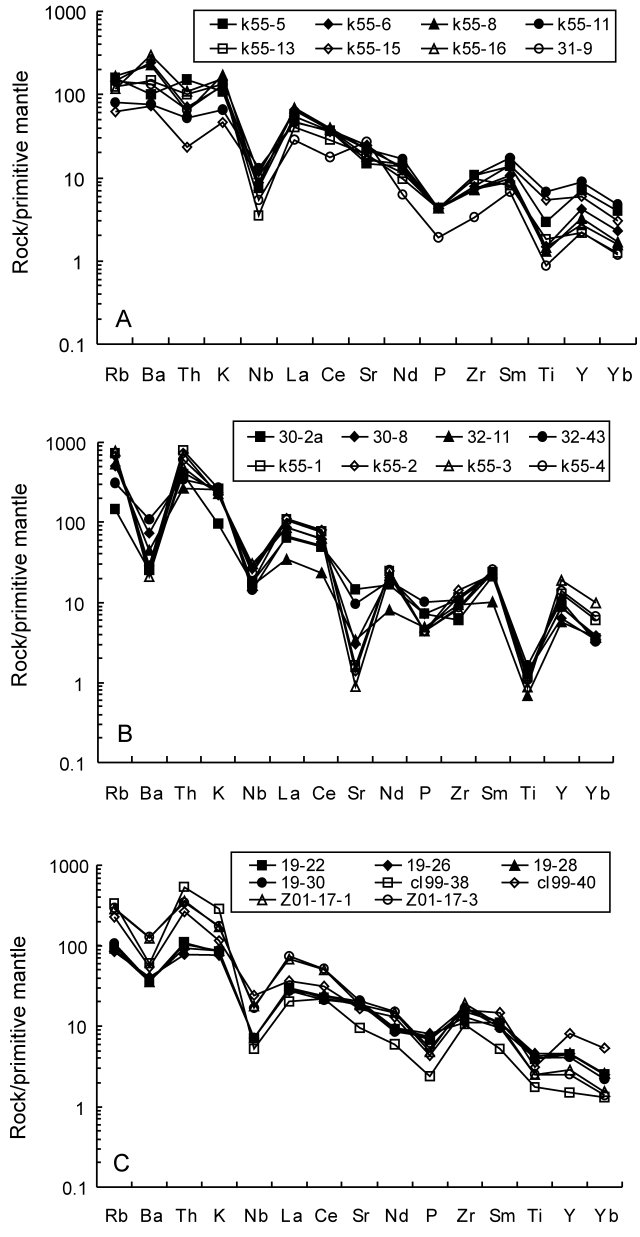

FIG. 3. Mantle-normalized trace-element patterns of North Qaidam granitoids. A, B, and C represent series 1, 2, and 3, respectively (primitive mantle values from Sun and McDonough, 1989).

the first series show obvious negative Nb, P, and Ti anomalies and positive Ba anomalies, suggesting an arc affinity. The granites of the second series also have negative Ba and Sr anomalies and positive Th anomalies. Muscovite granites have much larger Ba, Sr, and Th anomalies than do the biotite granites and orthogranites, which supports their interpretation as S-type granites. Rocks of the third series are characterized by obvious negative Y, Ba, Nb, P, and Ti anomalies of Ba and positive Th anomalies.

Zircon SHRIMP Dating

To determine the ages of the three granitoids series, we extracted zircons from samples collected from the Aolaoshan granite (K55-5), the Qaidamshan granite (K55-4), and the Dulan granite (CL99-40) for SHRIMP dating.

Analytical methods

Two-kg samples of rock were crushed to 80–120 mesh. After washing and drying, magnetic minerals were removed with a magnet, and zircon separated with heavy liquids. Individual grains of zircon were then hand picked under a binocular microscope. Grains of the selected zircon and two standard samples were mounted on a glass slide, polished and coated with ~10 nm of gold. Before coating, the zircons were photographed in transmitted light and imaged by cathodoluminescence (CL) to identify cores and rims. The SHRIMP dating was carried out by the first author in the SHRIMP Laboratory of Stanford University, USA. All data were collected on the SHRIMP-RG (sensitive high-resolution ion microprobe–reverse geometry) ion microprobe. Analytical spots ~30 um in diameter were sputtered using a 10 nA O_2- primary beam. The primary beam was rastered across the analytical spot for 90 seconds before analysis to reduce common Pb, and the resulting analyses show ^{204}Pb is generally <0.01 modal% of the total. Concentration data were standardized against the Sri Lankan zircon standard SL-13 and Duluth Gabbro zircon standard AS57; isotope ratios were calibrated against AS57, with an assumed age of 1099 Ma (Paces and Miller, 1993). Data reduction followed procedures described by Williams (1997). Errors on concordia intercepts were calculated at the 95 modal% confidence level.

Sample description

Sample K55-5. This sample was collected from the Aolaoshan pluton about 80 km northwest of Da Qaidan (Fig. 1). The intrusive body is an irregular stock with an outcrop area of 15 km^2, and was emplaced in Proterozoic gneiss and schist (Pt_3). The sample is light grey with an inequigranular granitic texture and a massive to gneissic structure. It consists of plagioclase (30–45 modal%), potassium feldspar (10–30 modal%), quartz (15–25 modal%), hornblende (0–10 modal%), and biotite (2–5 modal%). Some quartz has undulatory extinction, indicating plastic strain. Geochemically, the rock belongs to the first series of granitoids.

Sample K55-4. Sample K55-4 was taken from the Qaidamshan granite, located north of Da Qaidan (Fig. 1). The intrusive body is slightly elliptical, about 50 km long and 40 km wide, and has an area of 2124 km^2. Most of the body is covered with Quaternary deposits, but a good intrusive contact is exposed on its western margin, where this sample was collected (Fig. 1). The rock is coarse grained, with large phenocrysts of K-feldspar (20–40 modal%) up to 30 mm in length. The groundmass has an average grain size between 5 and 10 mm, and consists of K-feldspar, quartz, plagioclase, and biotite. Accessory minerals are corundum, tourmaline, fluorite, zircon, apatite, and cassiterite. The quartz grains are somewhat elongate, and the biotite has been mostly replaced by chlorite. The Qaidamshan granite is part of the second series of granitoids.

Sample CL99-40. This sample is from the Yematan granite, an irregular batholith that crops out over an area of 120 km^2 about 40 km north of Dulan (Fig. 1). The batholith exhibits sharp contacts with Proterozoic gneiss (Pt_3). The rock is coarse grained, with a hypidiomorphic- to allotriomorphic-granular texture. It consists of plagioclase (35–50 modal%), K-feldspar (15–20 modal%), quartz (10–15 modal%), hornblende (0–10 modal%), biotite (5–10 modal%), and accessory zircon and apatite.

Character of the zircons and SHRIMP dating results

Sample K55-5. Six zircons from Sample K55-5 were selected for SHRIMP dating (Table 2). As seen in Figure 4A, grains 1, 2, and 5 are short, subrounded prisms, whereas grains 3, 4, and 6 have irregular shapes. The inner structure of these zircons is very complicated, as revealed in the cathodoluminescence (CL) images (Fig. 4B). Grains 1, 2, 4, and 5 contain well-defined cores, but grain 4 differs from the others in having a white core with a sharp margin. The other three grains have irregular polygonal cores and a zoned rim, features considered to reflect partial melting or anatexis of the source rock (Robb et al., 1999; Keppie and Krogh, 1999). Grains 3 and 6 lack distinct cores and have slightly concentric oscillatory zoning, whereas grain 4 has distinct, concentric oscillatory zoning from core to rim (Fig. 4). The concentric zoning is considered evidence of a magmatic origin (Hanchar and Miller, 1993), and the internal structure of grain 4 suggests formation in a fluid-rich environment (Keay et al., 1999).

TABLE 2. U-Th-Pb SHRIMP Isotopic Data for Zircons of North Qaidam Granitoids[1]

Labels	U (ppm)	Th (ppm)	Th/U	^{204}Pb (ppb)	^{206}Pb	^{208}Pb/^{206}Pb	±	^{208}Pb/^{232}Th	±	^{206}Pb/^{238}U	±	^{207}Pb/^{235}U	±	^{207}Pb/^{206}Pb	±	^{206}Pb/^{238}U (Age)	±
K55-1.1	282	133	0.47	17	0.0163	0.1540	0.0106	0.0249	0.0018	0.0765	0.0016	0.5992	0.0473	0.0568	0.0042	475	10
K55-2.1	217	120	0.55	5	0.0061	0.1652	0.0071	0.0239	0.0011	0.0800	0.0013	0.6054	0.0259	0.0549	0.0021	496	8
K55-3.1	1887	563	0.30	5	0.0008	0.0905	0.0012	0.0227	0.0004	0.0749	0.0009	0.5742	0.0093	0.0556	0.0005	466	5
K55-4.1	99	59	0.60	9	0.0264	0.1700	0.0178	0.0204	0.0023	0.0716	0.0025	0.4840	0.0718	0.0490	0.0069	446	15
K55-5.1	714	236	0.33	1	0.0002	0.1048	0.0029	0.0253	0.0008	0.0797	0.0010	0.6145	0.0116	0.0559	0.0007	494	6
K55-6.1	225	85	0.38	8	0.0103	0.1099	0.0090	0.0216	0.0019	0.0744	0.0019	0.5495	0.0441	0.0535	0.0039	463	11
K554-1.1	134	88	0.66	1	0.0034	0.2038	0.0092	0.0204	0.0020	0.0657	0.0050	0.4878	0.0540	0.0539	0.0039	410	30
K554-2.1	3207	437	0.14	1	0.0001	0.0367	0.0016	0.0216	0.0026	0.0803	0.0078	0.6335	0.0765	0.0572	0.0035	498	47
K554-3.1	841	236	0.28	5	0.0017	0.0897	0.0036	0.0227	0.0010	0.0711	0.0009	0.5529	0.0178	0.0564	0.0016	443	5
K554-4	351	130	0.37	2	0.0017	0.1159	0.0073	0.0219	0.0014	0.0698	0.0009	0.5269	0.0313	0.0547	0.0031	435	6
K554-5.1	985	290	0.29	1	0.0004	0.0942	0.0019	0.0229	0.0006	0.0714	0.0009	0.5523	0.0134	0.0561	0.0011	445	5
K554-6.1	270	135	0.50	0	0.0002	0.1565	0.0051	0.0230	0.0010	0.0733	0.0018	0.5829	0.0227	0.0577	0.0016	456	11
K554-7.1	271	108	0.40	1	0.0014	0.1282	0.0046	0.0227	0.0009	0.0704	0.0012	0.5302	0.0220	0.0546	0.0020	438	7
K554-8.1	969	166	0.17	2	0.0007	0.0542	0.0015	0.0230	0.0007	0.0728	0.0010	0.5596	0.0204	0.0558	0.0018	453	6
K554-9.1	356	444	1.25	3	0.0022	0.3781	0.0099	0.0222	0.0011	0.0732	0.0027	0.5547	0.0320	0.0550	0.0022	455	16
K554-10.1	269	139	0.52	1	0.0004	0.1739	0.0034	0.0401	0.0015	0.1197	0.0030	1.1022	0.0419	0.0668	0.0017	729	17
K554-10.2	4218	871	0.21	23	0.0014	0.0540	0.0015	0.0208	0.0007	0.0796	0.0012	0.6100	0.0125	0.0556	0.0006	494	7
CL9940-1.1	262	176	0.67	–1	–0.0012	0.2247	0.0180	0.0205	0.0033	0.0614	0.0068	0.4889	0.0651	0.0577	0.0035	384	42
CL9940-2.1	209	102	0.49	–3	–0.0054	0.1687	0.0252	0.0216	0.0033	0.0623	0.0019	0.5101	0.0913	0.0594	0.0102	390	12
CL9940-3.1	572	377	0.66	0	0.0002	0.2262	0.0157	0.0193	0.0062	0.0562	0.0145	0.3917	0.1101	0.0505	0.0043	353	89
CL9940-4.1	415	288	0.69	1	0.0006	0.2252	0.0031	0.0204	0.0004	0.0628	0.0006	0.4647	0.0117	0.0537	0.0012	393	4
CL9940-5.1	454	197	0.43	0	0.0002	0.1409	0.0031	0.0207	0.0006	0.0638	0.0012	0.4759	0.0196	0.0541	0.0019	398	7
CL9940-6.1	640	407	0.64	1	0.0004	0.1993	0.0040	0.0195	0.0005	0.0623	0.0009	0.4528	0.0120	0.0527	0.0011	390	5
CL9940-7.1	454	202	0.44	1	0.0006	0.1367	0.0056	0.0193	0.0009	0.0627	0.0014	0.4564	0.0266	0.0528	0.0027	392	8
CL9940-8.1	382	231	0.60	–1	–0.0005	0.1919	0.0044	0.0193	0.0006	0.0606	0.0011	0.4791	0.0162	0.0574	0.0015	379	7
CL9940-9.1	636	244	0.38	0	0.0002	0.1174	0.0016	0.0198	0.0004	0.0646	0.0009	0.4809	0.0111	0.0540	0.0009	404	6
CL9940-10.1	179	86	0.48	0	0.0002	0.1500	0.0050	0.0203	0.0008	0.0648	0.0012	0.4922	0.0179	0.0551	0.0016	405	7
CL9940-11.1	564	304	0.54	2	0.0010	0.1722	0.0049	0.0205	0.0007	0.0640	0.0009	0.4656	0.0136	0.0528	0.0013	400	5
CL9940-12.1	233	129	0.55	3	0.0037	0.1711	0.0069	0.0199	0.0010	0.0645	0.0015	0.4695	0.0364	0.0528	0.0038	403	9
CL9940-13.1	489	187	0.38	0	0.0002	0.1237	0.0024	0.0210	0.0006	0.0650	0.0012	0.4873	0.0128	0.0544	0.0009	406	7
CL9940-14.1	216	100	0.46	7	0.0097	0.1376	0.0168	0.0196	0.0024	0.0659	0.0010	0.5194	0.0665	0.0572	0.0072	411	6

[1]The first author completed the zircon SHRIMP dating at Stanford University, USA. Data error is ±1σ.

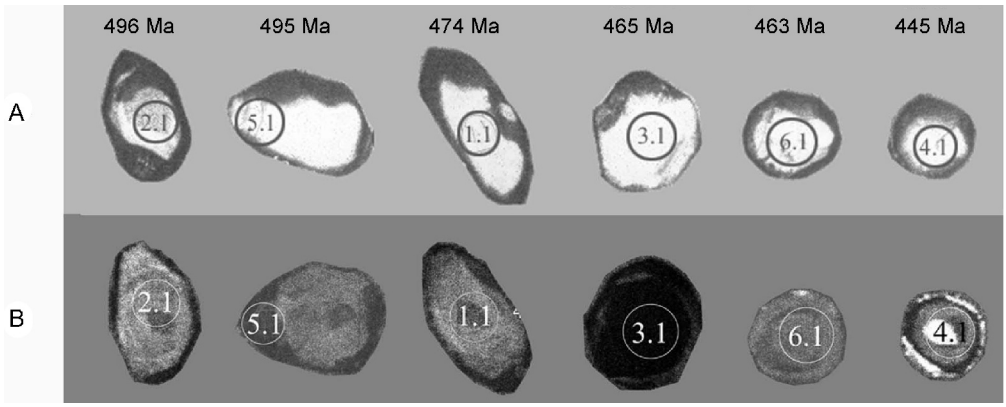

FIG. 4. Transmitted light (A) and cathodoluminescence(B) images of zircons from Aolaoshan, North Qaidam.

Based on the internal structure of the grains from sample K55-5, we suggest that the ages measured for grains 2, 4, and 5 represent the time of partial melting of a granitic protolith (496–474 Ma), and that grains 1, 3, and 6 represent later magmatic crystallization of the zircon (465–445 Ma). The zircons have U and Th contents ranging from 99.3 to 1887.1 ppm and from 59.2 to 236 ppm, respectively, and Th/U ratios ranging from 0.30 to 0.60. A comparison of compositions with CL images shows that the darker the image, the higher the U content. For instance, grain 3, which is black in the CL image, has a U content of 1887.1 ppm (Fig. 4). In contrast, grain 4, which has a white core, has a U content of only 99.3 ppm, which may indicate some loss of Pb (Claesson et al., 2000). Generally speaking, zircons with rounded shapes, high U contents, and low Th/U ratios (<0.1) are metamorphic in origin (Williams, 1995; Keay, et al., 1999; Robb et al., 1999), whereas those with Th/U ratios greater than 0.5 are regarded as being magmatic (Claesson et al., 2000; Hoskin and Black, 2000). Using these criteria, we concluded that all of the zircons from the Aolaoshan pluton are magmatic in origin.

Sample K55-4. Most of zircons from sample K55-4 have good prismatic and pyramidal forms, with length/width ratios between 2.5:1 and 1.5:1 (Fig. 5, A1 and A2). Some grains have cracks (Fig. 5, B1—1.1) or inclusions (Fig. 5, B2—7.1). In CL images, most of these zircons show obvious concentric oscillatory zoning from core to rim (Fig. 5, B1 and B2), indicating that they formed by magmatic crystallization (Vavra, 1990; Paterson et al., 1992). Again, grains that are light in color in the CL images have low U and high Th/U ratios (Table 2). For example, grain 1, which is light in color, has 134 ppm U, 10 ppm Pb, and a Th/U ratio of 0.66. Conversely, grains 2 and 10, which are the darkest in this sample, have much higher U and Pb contents (3207–4218 ppm and 242–320 ppm, respectively), but significantly lower Th/U ratios (0.14–0.21). Zircons having dark rims with Th/U ratios between 0.1 and 0.5, such as grains 2 and 10, may have been modified by late fluids (Pidgeon et al., 1998). Such fluid/grain interaction will typically cause an increase in the apparent age of the grains by the addition of radioactive Pb (Pidgeon et al., 1998).

The measured zircon ages for sample K55-4 range from 410 to 729 Ma (Table 2). Spot 10.1, which is the oldest age measured, is obviously located in an inherited zircon core based on its CL image and its high $^{207}Pb/^{206}Pb$ (Paterson et al., 1992). Spots 2.1 and 10.2 have ages of 498 Ma and 494 Ma, respectively, and these points are located in the dark margins of the grains, where the U content is high. Because the addition of radioactive Pb increases the measured age, these points are not included in the average age calculation. Ages for all the other zircons from this sample except for spot 1.1 have a relatively narrow range from 435 Ma to 456 Ma, and an average age of 446 Ma (standard deviation of 7.7 Ma). This age should reflect the time of crystallization of the granitic body because these zircons all have obvious concentric zoning (Vavra, 1990; Paterson et al., 1992). The lower age of spot 1.1 may reflect loss of Pb because the grain has an obvious crack.

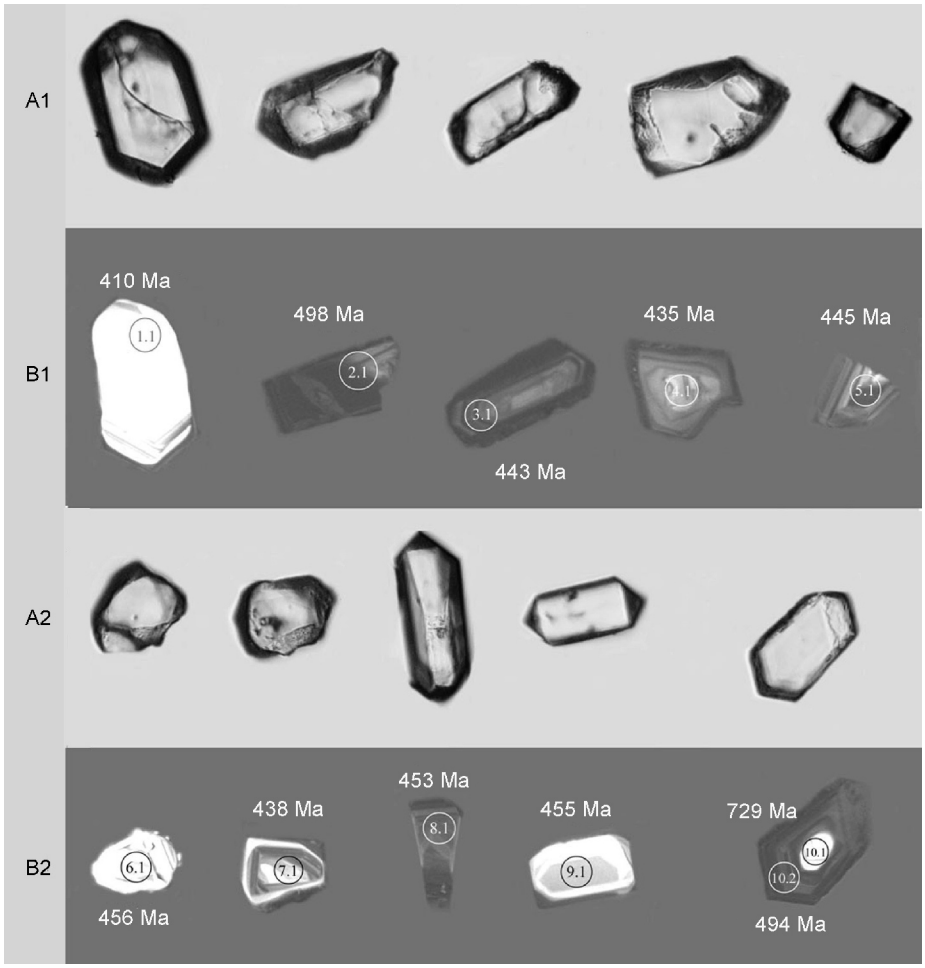

FIG. 5. Transmitted light (A) and cathodoluminescence (B) images of zircons from Qaidamshan, North Qaidam.

Sample CL99-40. Fourteen zircon grains from sample CL99-40 were dated. All of the zircons have good crystal forms with pyramidal and prismatic faces, and length/width ratios of 3.5:1–1.5:1. Most of the zircons show obvious zoning and some contain mineral inclusions (Fig. 6). Uranium contents range from 179 to 640 ppm, Th contents from 86 to 407 ppm, and Th/U ratios are all greater than 0.5, indicating crystallization from a granitic magma. The measured ages range from 379 ± 7 Ma to 411 ± 6 Ma, and average 397 ± 4.2 Ma (Fig. 7). Except for spot 3.1 (353 ± 89 Ma), all the measured ages have high precision. Based on the character of the zircons, the measured ages are taken as the crystallization age of the granitic body.

Discussion

Tectonic environments in which the granitoids formed

The granitoids as a whole define a belt that is aligned at a small angle to the regional tectonic trend. Some of the bodies have well-developed foliations at the margins formed by the preferred orientation of biotite grains. The intrusive rocks consist chiefly of granite, granodiorite, and quartz diorite. Ordovician volcanic rocks are also present, and occur in a NW-trending belt that lies southwest of the plutonic rocks. The volcanic rocks consist of olivine tholeiite, olivine trachyandesite, basaltic andesite, andesite, dacite and rhyolite. Most of the

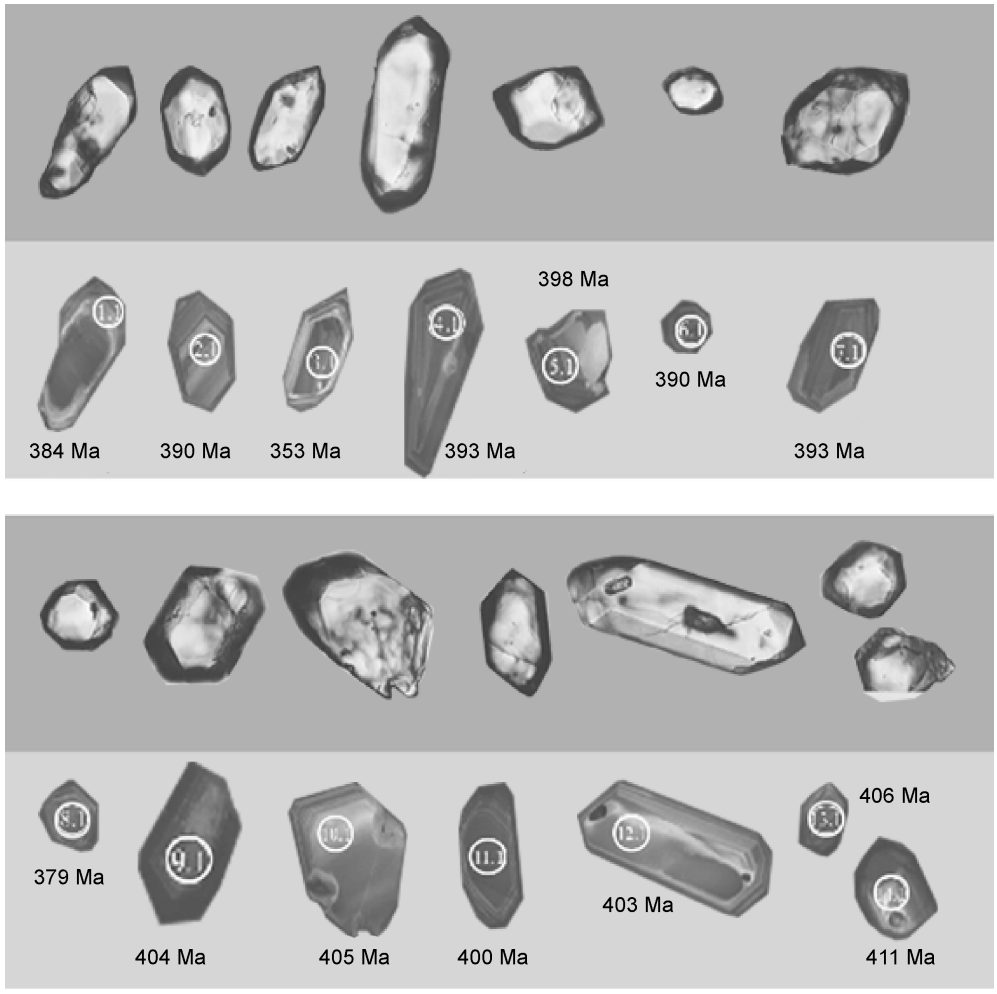

FIG. 6. Transmitted light (A) and cathodoluminescence (B) images of zircons from Yematan, Dulan, North Qaidam.

volcanic rocks are calc-alkaline in character, but both tholeiitic and Na-rich alkalic varieties are present. The compositions of these rocks suggest formation at oceanic spreading centers and in arc environments, which in turn suggests that they formed during the opening and closing of an Ordovician ocean basin (Qiu et al., 1998).

Based on a study of early Paleozoic North Qaidam volcanic rocks, Qiu et al. (1998) postulated the presence of a small oceanic basin in North Qaidam. He found that early Paleozoic mafic and silicic volcanic rocks are tholeiitic and mildly alkalic, indicating formation in an oceanic basin, whereas those of middle to late Paleozoic age are intermediate to mafic in character, suggesting that they formed during closure of the basin. A zircon U-Pb age of 496.3 ± 6.2 Ma for the Luliangshan gabbros in North Qaidam indicates an Early Ordovician magmatic event (Yuan et al., 2002). Yuan et al. suggested that the gabbros were formed by partial melting of a depleted mantle source, and that they are part of an island arc suite generated along the active continental margin of North Qaidam. This suggests that eruption of the island arc volcanic rocks of North Qaidam and subduction of the Qaidam block occurred prior to the Early Ordovician.

The three granitoids suites discussed in this paper were formed in the Early Ordovician, Middle

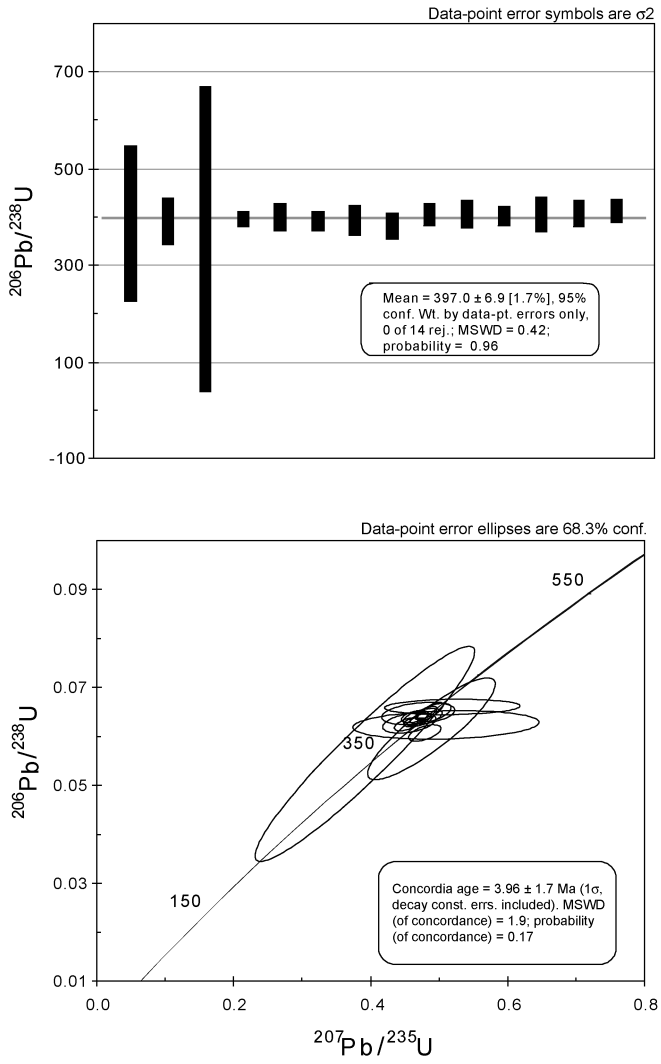

FIG. 7. U-Pb concordia diagram showing age data of SHRIMP U-Pb zircon dating from Yematan, Dulan, North Qaidam.

to Late Ordovician, and Early Devonian. The first suite consists of I-type granitic similar to those formed in island arc environments, the second series is typical of syn-collisional granites, and the third is intermediate in character between island arc and sys-collisional plutonic rocks. On trace-element spider diagrams (Fig. 8), rocks of the first series have higher contents of K, Rb, Ba, and Th and lower contents of Ta, Nb, Ce, Hf, Zr, Sm, Y, and Yb than ocean ridge granites. They also have notable negative Ta and Hf anomalies, characteristic features of island-arc or active continental margin plutonic rocks. The second series is characterized by positive Rb and Th anomalies and negative Ba and Hf anomalies and has K, Rb, Ba, Th, Ta, Nb and Ce contents similar to those of syn-collisional granites. The third series has a very complicated composition, with K, Rb, Ba, and Th higher than ocean-ridge granites, but with positive Rb and Th anomalies and variable Hf, Zr, Sm, Y, and Yb contents. The third series appears to have inherited compositional features from both the first and second series. Based on their

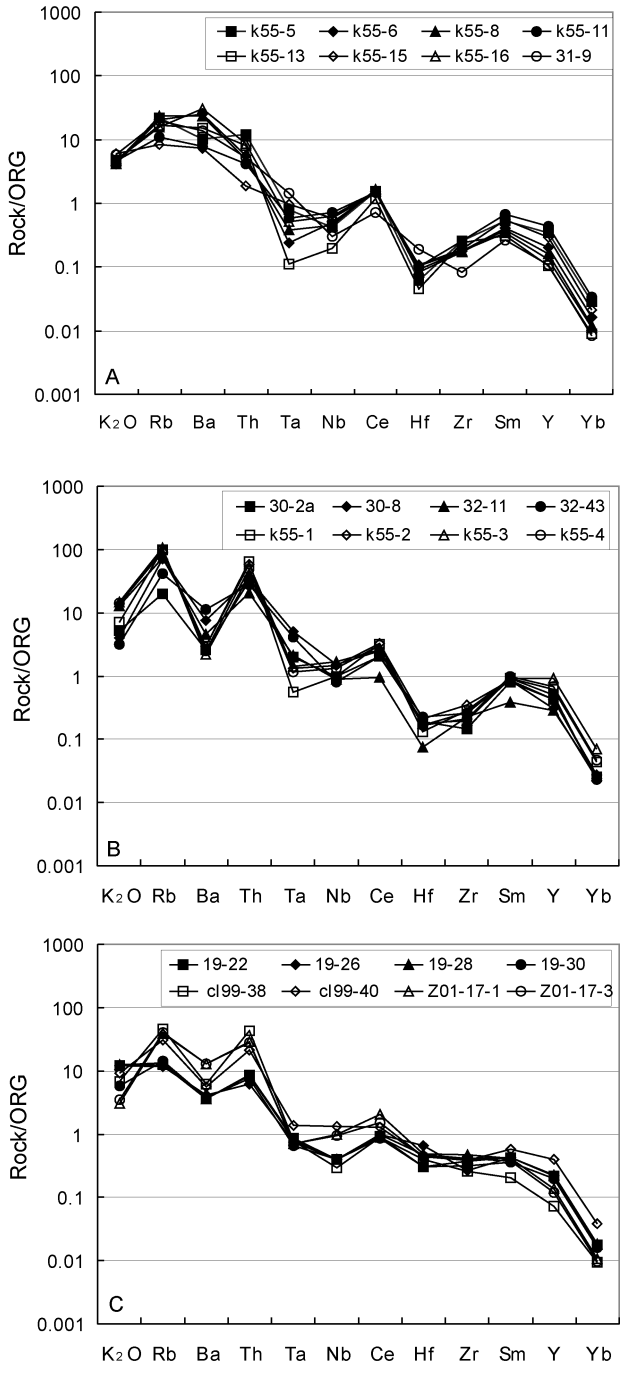

FIG. 8. Ocean-ridge granite (ORG)–normalized patterns of granitoids from North Qaidam. Normalizing data of ORG are from Pearce et al (1984).

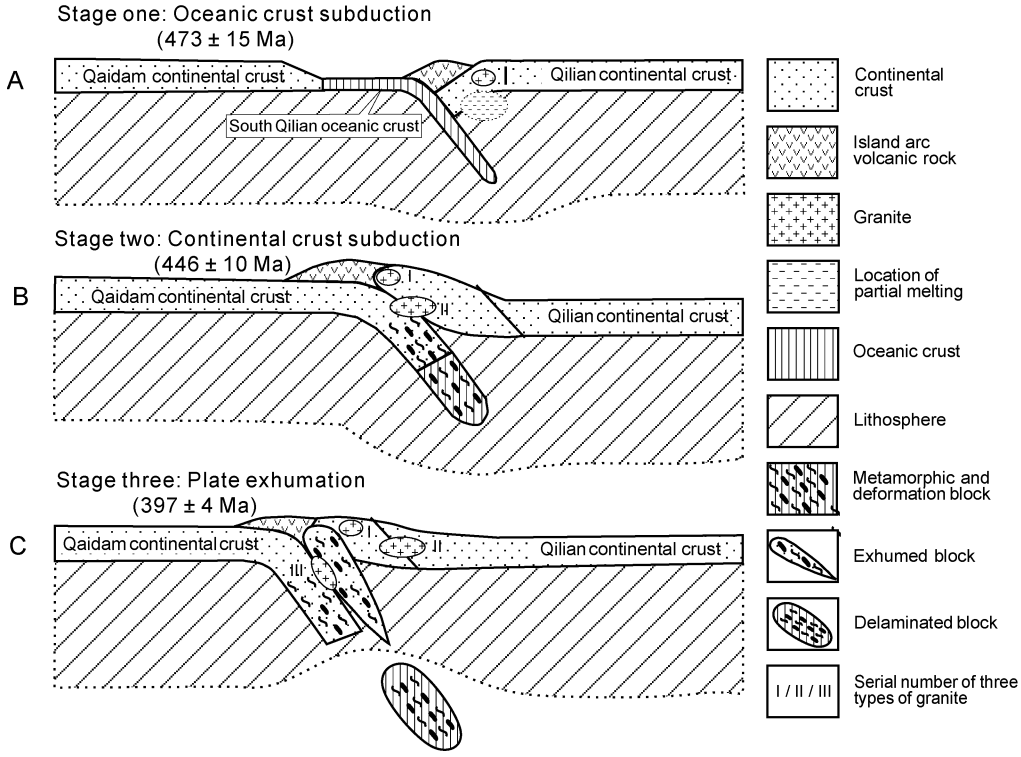

FIG. 9. Diagram showing early Paleozoic interpreted tectonomagmatic evolution of North Qaidam.

composition and age, these rocks are believed to be part of a post-orogenic association.

Ultrahigh-pressure metamorphism and the timing of exhumation

Zhang et al. (2000) have shown that eclogite from Yuka of Da Qaidan has a zircon ^{238}U-^{206}Pb age of 494.6 ± 6.5 Ma, representing the time of peak metamorphism. Phengite in the eclogite has an ^{40}Ar-^{39}Ar age of 466.7 ± 1.2 Ma and an isochron age of 465.9 ± 5.4 Ma, representing retrograde metamorphism of the eclogite during cooling. The gneiss hosting the eclogite is dated at 477.7± 17.7 Ma (Zhang et al., 2000). Hao et al. (2001) reported an age of 484 ± 3 Ma for a similar eclogite at Saliuhe. Based on these ages, UHP metamorphism on the northern margin of the Qaidam Range occurred roughly between 494 and 466 Ma. The ages of the first and second series of granitoids overlap the time of UHP metamorphism, indicating a close relationship between metamorphism and plutonism.

Coesite inclusions in zircon from granitic gneiss at Dulan indicate that the gneiss also underwent UHP metamorphism. The Dulan gneiss has a muscovite Ar-Ar age of 401.5 ± 0.5 Ma (Yang et al., 2001), and another granitic gneiss at Xitieshan has a similar muscovite Ar-Ar age of 405.7 ± 0.9 Ma (Xu et al., 2003). These ages are taken to represent exhumation of the UHP metamorphic rocks to depths of ~10 km (Xu et al., 2003). These ages are similar to those of the third series of granitoids, suggesting that these plutonic rocks formed during exhumation.

Stages of granitic magmatism

Paleozoic granitoids along the northern margin of Qaidam Basin can be divided into three series based on their age, geochemistry, and regional geological relationships. The first series consists of I-type granitic rocks formed during subduction of oceanic lithosphere northward under the South Qilian at the end of the Cambrian (Lai et al., 1996; Qiu et al., 1998). The subducted lithosphere was metamorphosed to the eclogite facies, resulting in release of abundant fluids during dehydration (cf. Peacock, 1990; Sorena and Jeffrey, 1993). The upward migra-

tion of these fluids caused partial melting of the upper mantle and lower crust to form I-type granitic magmas between 496 and 446 Ma (average 473 Ma). The eclogites within the belt also formed chiefly during this period (Fig. 9A).

Continent-continent collision occurred in the belt during closure of the Qaidam ocean basin, causing thickening of the crust. Partial melting of the thickened continental crust between 456 and 435 Ma (average 446 Ma) formed the S-type granites of the second series. This period of magmatism partly overlapped formation of eclogites in the region (Fig. 9B).

Deep subduction of the oceanic crust produced dense eclogites, leading to delamination of the lithospheric mantle. Delamination promoted upwelling of hot asthenosphere, causing heating of the lithosphere, and isostatic rebound of the low-density continental crust. Granitoids of the third series may have been produced by mixing of mantle melts with those formed by crustal anatexis (Milord et al., 2001). The age of these granitoids (411–379 Ma) corresponds to the time of crustal exhumation (Fig. 9C).

Conclusions

Paleozoic granitoids are widespread in North Qaidam, where they provide useful information on the tectonic evolution of the region. Three distinct compositional series have been recognized, with ages spanning ~75 m.y. The first series consists of quartz monzodiorite–granodiorite–monzogranite, the second of monzogranite–biotite + muscovite granite–muscovite granite, and the third of granodiorite-monzogranite-biotite granite. The first series consists of I-type granitic rocks formed in an island-arc or active-margin environment, with an average age of 473 Ma. These intrusive rocks formed during subduction of oceanic lithosphere in the Early Ordovician. As the ocean basin closed, continental crust of the Qaidam block was carried into the mantle where it was subjected to UHP metamorphism and partially melted to form S-type granites of the second series at about 446 Ma. The subducted oceanic lithosphere was converted to dense eclogites, which were then delaminated from the continental material. Upwelling of the asthenosphere and exhumation of the coesite-bearing felsic rocks caused partial melting of the continental lithosphere, forming the third series of post-collisional granitic rocks at about 397 Ma.

Acknowledgments

This work was financially supported by the Chinese Natural Science Foundation of China Project (40472034), the Chinese National Key Project for Basic Research (2003CB716500), the National 973 Project (G1988040800), and China Geological Survey Project (200313000058). We thank Li Ronghua, Huang Xuan, Pan Jun, Xu Ping, and Han Xiuling for their help with the whole-rock chemical analyses, microprobe analyses, and isotopic analyses.

REFERENCES

Boynton, W. V., 1984, Cosmochemistry of the rare earth elements. Meteorite studies: Developments in Geochemistry, v. 2, p. 63–114.

BGMRQH (Bureau of Geology and Mineral Resource, Qinghai Province), 1991, Regional geology of Qinghai province: Beijing, China, Geological Publishing House, 662 p. (in Chinese).

Claesson, S., Vetrin, V., Bayanova, T., and Downes, H., 2000, U-Pb zircon ages from a Devonian carbonatite dyke, Kola peninsula, Russia: A record of geological evolution from the Archaean to the Palaeozoic: Lithos, v. 51, p. 95–108.

Hanchar, J. M., and Miller, C. F., 1993, Zircon zonation patterns as revealed by cathodoluminescence and backscattered electron images: Implications for interpretation of complex crustal histories: Chemical Geology, v. 110, p. 1–13.

Hao, G., Lu, S., Li, H., and Zheng, J., 2001, Determination and significance of eclogite on Shalihe, in the north margin of Qaidam Basin: Progress in Precambrian Research, v. 24, no. 3, p. 154–162.

Hoskin, P. W. O., and Black, L. P., 2000, Metamorphic zircon formation by solid-state recrystallization of protolith igneous zircon: Journal of Metamorphic Geology, v. 18, p. 423–439.

Irvine, I. N., 1971, A guide to the chemical classification of the common volcanic rocks: Canadian Journal of Earth Sciences, v. 8, p. 532–548.

Keay, S., Steele, D., and Compston, W., 1999, Identifying granite sources by SHRIMP U-Pb zircon geochronology: An application to the Lachlan fold belt: Contributions to Mineralogy and Petrology, v. 137, p. 323–341.

Keppie, D. J., and Krogh, T. E., 1999, U-Pb Geochronology of Devonian granites in the Meguma terrane of Nova Scotia, Canada: Evidence for hotspot melting of a Neoproterozoic source: Journal of Geology, v. 107, p. 555–568.

Lai, S., Deng, J., and Zhao, H., 1996, Volcanism and tectonic setting during Ordovician period on north margin of Qaidam: Journal of Xi'an College of Geology, v. 18, no. 3, p. 8–14 (in Chinese).

Milord, I., Sawyer, E. W., and Brown, M., 2001, Formation of diatexite migmatite and granite magma during anatexis of semi-pelitic metasementary rocks: An example from St. Malo, France: Journal of Petrology, v. 42, no. 3, p. 487–505.

Paces, J. B., and Miller, J. D., 1993, U-Pb ages of the Duluth complex and related mafic intrusions, northeastern Minnesota: Geochronologic insights into physical petrogenetic, paleomagnetic, and tectonomagmatic processes associated with the 1.1 Ga mid-continent rift system: Journal of Geophysical Research, v. 98, p. 13,997–14,013.

Paterson, B. A., Stephens, W. E., Rogers, G., Williams, I. S., Hinton, R. W., and Herd, D. A., 1992, The nature of zircon inheritance in two granite plutons: Transactions of the Royal Society of Edinburgh, Earth Science, v. 83, p. 459–471.

Peacock, S. M., 1990, Fluid processes in subduction zones: Science, v. 248, p. 329–337.

Pearce, J. A., Nigel, B. W. H., and Andrew, G. T., 1984, Trace element discrimination diagrams for the tectonic interpretation of granitic rocks: Journal of Petrology, v. 25, p. 956–983.

Pidgeon, R. T., Nemchin, A. A., and Hitchen, G. J., 1998, Internal structures of zircons from Archaean granites from the Darling Range batholith: Implications for zircon stability and the interpretation of zircon U-Pb ages: Contributions to Mineralogy and Petrology, v. 132, p. 288–299.

Qiu, J., Yang, W., and Xia, W., 1998, The early Palaeozoic Marine volcanic rocks and ore-forming condition and prospecting directions, *in* Xia Linqi, Xia Zuchun, Ren Youqiang, Zuo Guocao, and Qiu Jiaxiang, eds., Volcanism and ore-forming in Qilianshan and adjacent areas: Beijing, China, Geological Publishing House, p. 111–163 .

Robb, L. J., Armstrong, R. A., and Waters, D. J., 1999, The history of granulite-facies metamorphism and crustal growth from single zircon U-Pb geochronology: Namaqualand, South Africa: Journal of Petrology, v. 40, no. 12, p. 1747–1770.

Song, S. G., Yang, J. S., Liou, J. G., and Shi, R. D., 2003a, Metamorphic evolution of coesite-bearing ultrahigh-pressure terrane in the North Qaidam, Northern Tibet, NW China: Journal of Metamorphic Geology, v. 21, no. 6, p. 631–644.

Song, S. G., Yang, J. S., Liou, J. G., and Xu, Z. Q., 2003b, Petrology, geochemistry, and isotopic ages of eclogites from the Dulan UHPM Terrane, the North Qaidam, NW China: Lithos, v. 70, p. 195–211.

Sorena, S. S., and Jeffrey, N. G., 1993, Accessory minerals and subduction zone metasomatism: A geochemical comparison of two mélanges: Chemical Geology, v. 110, p. 269–297.

Sun, S. S., and McDonough, W. F., 1989, Chemical and isotopic systematics of oceanic basalts: Implications for mantle composition and processes, *in* Saunders, A. D., and Norry, M. J., eds., Magmatism in the ocean basins: Geological Society of London, Special Publication, v. 42, p. 313–345.

Vavra, G., 1990, On the kinematics of zircon growth and its petrogenetic significance: A cathodoluminescence study: Contributions to Mineralogy and Petrology, v. 106, p. 90–99.

Williams, I. S., 1995, Zircon analysis by ion microprobe: the case of the eastern Australian granites, *in* Leon, T., ed., Silver 70th birthday symposium and celebration: Pasadena, CA, The California Institute of Technology, p. 27–31.

Williams, I. S., 1997, U-Th-Pb geochronology by ion microprobe: Not just ages but histories, *in* McKibben, M. A., Shanks, W. C., III, and Ridley, W. I., eds., Applications of microanalytical techniques to understanding mineralizing processes: Reviews of Economic Geology, v. 7, p. 1–35.

Xu, Z., Yang, J., Wu, C., Li, H., Zhang, J., Qi, X., Song, S., Wan, Y., Chen, W., and Qiu, H., 2003, Timing and mechanism of formation and exhumation of the Qaidam ultrahigh pressure metamorphic belt: Acta Geologica Sinica, v. 77, no. 2, p. 163–176.

Yang, J., Song, S., Xu, Z., Wu, C., Shi, R., Zhang, J., Li, H., Wan, Y., Liu, Y., Qiu, H., Liu, F., and Shigenori, M., 2001, Discovery of coesite in the north Qaidam early Paleozoic ultrahigh-high pressure (UHP-HP) metamorphic belt, NW China: Acta Geologica Sinica, v. 75, no. 2, p. 175–179 (in Chinese).

Yang, J., Xu, Z., Li, H., Wu, C., Zhang, J., and Chen, W., 1998, Discovery of eclogite at the northern margin of Qaidam Basin, NW China: Chinese Science Bulletin, v. 43, p. 1755–1760.

Yang, J., Xu, Z., Song, S., Wu, C., Shi, R., Zhang, J., Wan, Y., Li, H., Jin, X., and Marc, J., 2000, Discovery of eclogite in Dulan, Qinghai Province and its significance for studying the HP-UHP metamorphic belt along the central orogenic belt of China: Acta Geologica Sinica, v. 74, no. 2, p. 156–168 (in Chinese).

Yang, J., Xu, Z., Zhang, J., Song, S., Wu, C., Shi, R., Li, H., and Maurice, B., 2002, Early Palaeozoic North Qaidam UHP metamorphic belt on the north-eastern Tibetan plateau and a paired subduction model: Terra Nova, v. 14, p. 397–404.

Yuan, G., Wang, H., Li, H., Hao, G., Xin, H., Zhang, B., Wang, Q., and Tian, Q., 2002, Zircon U-Pb age of the gabbros in Luliangshan area on the northern margin of Qaidam Basin and its geological implication: Progress in Precambrian Research, v. 25, no. 1, p. 36–40.

Zhang, J., Yang, J., Xu, Z., Zhang, Z., Chen, W., and Li, H., 2000, Peak and retrograde age of eclogites at the northern margin of Qaidam basin, northwestern China: Evidence from U-Pb and Ar-Ar dates: Geochimica, v. 29, no. 3, p. 217–222.

Zhang, J. X., Zhang, Z. M., Xu, Z. Q., Yang, J. S., and Cui, J., 1999, The ages of Sm-Nd and U-Pb of eclogite from the west Altyn tectonic belt: Chinese Science Bulletin, v. 44, p. 1109–1112 (in Chinese).